

Nanoparticle Effects of Thermoplastic Polyurethane on Kinetics of Microphase Separation, With or Without Preshear

Iman Sahebi Jouibari , Milad Kamkar, Hossein Nazokdast

Department of Polymer Engineering and Color Technology, Amirkabir University of Technology (Tehran Polytechnic), Tehran, Iran

The present research was carried out in two stages. First, various nanoparticles (Closite30B and multiwalled carbon nanotubes [MWCNTs]) for reinforcement of the polymer matrix were prepared and characterized. Samples were prepared with a melt mixing technique. In the next step, the kinetics of phase separation of thermoplastic polyurethane with nanoparticle (Closite30B, MWCNTs) and preshear were investigated by linear viscoelastic experiments, including frequency sweep and time sweep tests, which were performed on TPU/Closite30B/MWCNT samples varying in nanoparticle content at rheological measurements. The kinetics of phase separation at high preshear and a lower percentage of nanoparticles increased, while they showed a decrease in higher compositions. The nucleation effect of nanoparticles and the effect of preshear with the orientation of the hard segment increases the kinetics of phase separation of the soft and hard segments. The differential scanning calorimetry (DSC) showed that multiple endothermic peaks of thermoplastic polyurethane were affected in the presence of nanoparticles. Dynamic mechanical tests showed that Closite30B has greater affinity with the soft segment and MWCNTs with the hard segment, according to the DSC and rheological experiments. Finally, it was observed that the shear flow and nanoparticles can accelerate phase separation kinetics, but the effect of preshear on the kinetics of phase separation was reduced in the presence of a strong nucleating agent like MWCNTs. *POLYM. COMPOS.*, 00:000–000, 2017. © 2017 Society of Plastics Engineers

INTRODUCTION

Thermoplastic polyurethane (TPU) is one of the best tailoring polymers, which lets the user change its properties in an arbitrary manner. The final properties of TPUs depend on several parameters, such as their chemical nature, thermal history, and hydrogen bonds. These variables can control the final morphology. Hence, the

crystalline structure of the hard segment greatly influences the rheological and mechanical properties of the TPU [1–3].

In some TPUs, the hard segments are crystalline, and crystallinity is part of the driving force that leads to phase separation polymers [4, 5]. The chemical structures and morphologies of the hard segment exert a great effect on crystallization, for example, tolylene-2,6-diisocyanate butanediol (2,6-TDI-BD) and methylene diphenyl diisocyanate butanediol (MDI-BD) are capable of crystallization under proper conditions. The effects of temperature and annealing on hydrogen bonding and crystallization are surveyed with DSC [6].

Nanocomposites are a new class of materials having better physical properties, such as thermal, mechanical, and barrier properties, compared to conventional composites, because of the much stronger interfacial interaction between the well-dispersed nanometer-sized domains [7].

TPU nanocomposites present a fascinating system for study because of the already complex microphase structure of TPUs. Recent investigations have shown that layered silicates can have a significant impact on the microphase structure of block copolymers [8].

For example, in the presence of nano clay in polyurethane, there is an unchanged size of the hard domain, but it effect on the interdomain distance of the hard domain and the spherical aggregate domain. In the presence of clay, spherical aggregates decrease from 800 to 500 nm; it clearly has an effect on the mechanical properties of polyurethane [9].

Nanoparticles enhance the nucleation process as a nucleating agent, which results in an acceleration of the crystallization kinetics. The performance of these nucleating agents depends on many factors: type and concentration of nanoparticle, shape (symmetric or asymmetric), dispersion or agglomeration, its polarity, and the specific interactions with the polymer chain [10].

The flow field effect on the complex morphology of TPUs caused by the chain orientation—helps phase separation, causes the hard segments to move faster to each

Correspondence to: H. Nazokdast; e-mail: nazdast@aut.ac.ir

DOI 10.1002/pc.24563

Published online in Wiley Online Library (wileyonlinelibrary.com).

© 2017 Society of Plastics Engineers

other, and causes them to make the hard domain and aggregation earlier. Also, preshear at annealing temperatures between glass temperature and melt temperature of the TPUs implies a structural and morphological variation of hard domains, thereby increasing their phase separation [11–14].

Owing to the effect of the flow on nucleation phenomena and kinetic phase separation of TPUs, this has been the subject of many studies in the literature. Mourier et al. studied the effect of shear on a wide category of polyether- and polyester-based polyurethanes. Based on their research, phase separation kinetics of TPUs is increased in the presence of preshear in all samples in the range of phase separation temperatures with a wide range of preshear [15, 16].

The effect of the shear flow on the kinetics of polymer nanocomposite crystallization is a crucial issue in literature. The nanoparticles are usually assumed as a nucleating agent; also, shear flow decreases the entropy of the polymer chain and lets them be aligned, and promotes the kinetics of crystallization. Its difficulty is caused by the synergistic effect of shear flow and nanoparticle because, in the presence of nanoparticles, chain dynamics decrease in order to trap the chains on to the nanoparticle surface and prevent chain orientation. The distinction of these factors from each other depends on many factors like the type of nanoparticles, type and intensity of flow field (shear or elongation), and the concentration of nanoparticles [17].

TPUs hard domain assembly offers control over the microstructure and physical properties, considering nowadays the increasing versatile demands on high-performance materials [1, 18].

Rheology is a reliable method used to deduce the morphological features of complex fluids. Plenty of inquiries have been carried out to characterize polymeric nanocomposites using rheology. A few studies have reported the effect of organo clay on the microstructural development of melt-intercalated TPU nanocomposites [19]. Moreover, linear and nonlinear rheological characteristics of these nanocomposites were not studied well during thermal transitions. TPUs can exhibit a wide variety of transitional features, ranging from order-disorder transition (ODT) a typical feature of block copolymers to micro-phase separation and solidification [12, 13, 20, 21].

This study is mainly focused on the rheological properties and microstructural development of TPU/Cloisite30B/MWCNTs nanocomposites. Additionally, the effect of preshear on the kinetic phase separation in the presence of two nanoparticles with different affinities with the soft or hard segments discussed. The influence of this factor on phase separation of TPU nanocomposites, survey with rheological approach in addition to standard DSC and DMTA analyses.

EXPERIMENTAL

Materials

A polyester-based thermoplastic polyurethane (Desmopan 385A, $\rho = 1,200 \text{ (kg/m}^3\text{)}$), provided by Bayer Material

TABLE 1. Compounding formulation Cloisite 30B & MWCNT samples.

Sample	Cloisite 30B loading wt%	Sample	MWCNT loading wt%
CB1	0.15%	CNT1	0.1%
CB2	0.5%	CNT2	0.2%
CB3	1%	CNT3	0.4%
CB4	3%	CNT4	0.8%
CB5	5%	CNT5	1.2%
CB6	7%	CNT6	2%

Science AG, Germany), with a molecular weight of $M_n = 111,000 \text{ (g/mol)}$ and polydispersity index (PDI) of 1.46, was used as the polymer matrix. The soft segment comprised of polytetramethyleneadipate (PTMG), 1, 4-butanediol (BD) as the chain extender, and its hard segment was composed of 4,4'-methylendiphenil isocyanate (MDI), around 40% of the hard segment [20]. Organically modified clay Cloisite30B (CEC: 90 meq/100 g) was obtained from the southern clay product. The multiwall carbon nanotubes (MWCNTs), nanocyl 7000, with the average diameter of 9.5 nm, the average length of 1.5 μm , and purity of 90% supplied by nanocyl, were used as nanoparticles.

Sample Preparation

Two sets of TPU nanocomposite samples TPU/Cloisite30B and MWCNTs, each varying in Cloisite30B and MWCNTs content (ranging from 0.15 to 7 wt% for Cloisite30B and from 0.1 to 2.0 wt% for MWCNTs)—were prepared using the melt-compounding method using a laboratory internal mixer (Braebender Plasticorder W50). Melt-compounding was carried out in a 60 cm^3 at 210°C with rotor speed of 100 rpm for 18 min for Cloisite30B and 15 min for MWCNTs. In order for TPU and nanoparticles to have the ability to absorb moisture easily, TPU was dried before mixing at 80°C for 24 h, and nanoparticles were dried at 140°C for 12 h. The samples are coded in Table 1.

Characterization

DSC measurements were conducted on a Mettler Toledo system, under a nitrogen atmosphere, at a heating rate of 10°C/min an aluminum pan. The samples were heated at the rate of 10°C/min from room temperature to 210°C and then held isothermally for 5 min so that thermal history vanishes, and then cooled at the rate of 10°C/min to -50°C .

The dynamic mechanical properties of nanocomposites were measured using dynamic mechanical thermal analyzer Diamond DMA Perkin Elmer in the tensile mode at frequency of 1 Hz on molded samples (20 \times 11 \times 1 mm). The test was carried out at a frequency of 1 Hz, static force of 0.1 N, and the temperature range -80°C to

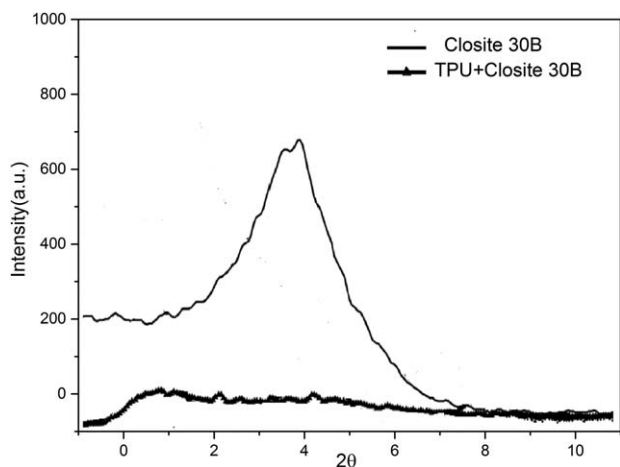


FIG. 1. XRD patterns of Cloisite30B and TPU nanocomposites containing 5 wt% of Cloisite30B.

150°C and a scan rate of 3°C/min under nitrogen atmosphere.

To measure the linear viscoelastic responses of TPU and the nanocomposite samples, a Rheometrics mechanical spectrometer (Paar Physica UDS200) equipped with a parallel plate fixture (25 mm diameter and a constant gap of 1 mm) was employed. The neat TPUs were heated for 15 and 5 min for nanocomposite samples in order to erase thermal history, residual stress, and hard domain in melt temperature [20]. The neat and nanocomposites were cooled rapidly to annealing temperature. This cooling process usually took 2 min for 50°C to 70°C drop in temperature. Then the storage modulus and the loss modulus (G' , G'') of the samples were measured by a time sweep experiment in order to study the microphase separation and hard domain aggregation, at an annealing temperature for 2 h. In order to investigate the effect of shear flow on phase separation kinetics, time sweep experiment was conducted at various preshears, ranging from $\gamma = 5$ to 30 1/s, before starting time sweep test at annealing temperature. Hard domain aggregation formed during the time sweep test of 2 h is evaluated by temperature sweep experiment in the heating process from annealing

temperature to 220°C. The mechanism of heating was conducted at a rate of 2°C/min for all the samples to find the ODT temperature [22]. The cooling process was carried out at the rate of 10°C/min for neat TPU and nanocomposites, because of which we can have a comparison with the DSC nucleating effects of nanoparticle and preshear.

RESULTS AND DISCUSSION

Morphological Characterization

Figure 1 shows XRD patterns of Cloisite30B, and the TPU containing 5% Cloisite30B. As can be seen, the characteristic peak of Cloisite30B, at $2\theta = 4.8$ (d -spacing = 1.85 nm), almost disappeared for the nanocomposites. This indicates that silicate layers of Cloisite30B are exfoliated or highly intercalated in the TPU matrix. The good dispersion of the silicate layers may be attributed to the specific interaction originating from the hydrogen bonding between urethane groups in TPUs and hydroxyl groups in nanoparticles.

MWCNTs and TPU have strong interactions, which have been reported in previous studies [20].

Rheological Behavior at Frequency Sweep Test

This article focused on a sample of nanocomposites Cloisite30B because previous works have discussed nanocomposite MWCNTs, and just that for use as supplementary information [20].

Figure 2a and b shows the storage modulus, G' , and complex viscosity, $|\eta^*|$, for neat TPU and the nanocomposites with different Cloisite30B contents in frequency sweep test in melt temperature. This test was carried out after erasing the thermal history to make all samples completely disordered. As can be observed, while the neat TPU exhibited a terminated G' at low-frequency range, the nanocomposite samples showed a very strong nonterminal G' and viscosity upturn in low frequency regions.

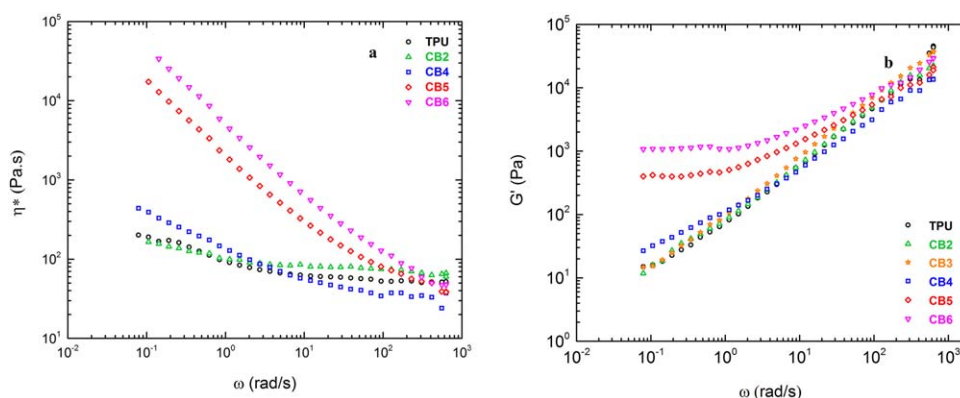


FIG. 2. Viscosity and storage modulus of TPU/Cloisite30B nanocomposite (a) viscosity versus frequency, (b) modulus versus frequency. [Color figure can be viewed at wileyonlinelibrary.com]

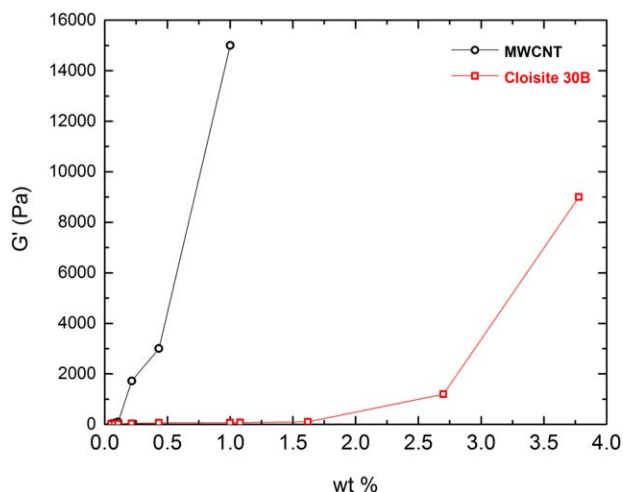


FIG. 3. Increase in storage modulus versus percentage of nanoparticles (Cloisite30B and MWCNT). [Color figure can be viewed at wileyonlinelibrary.com]

On reaching the percolation threshold (5% for Cloisite30B) and being independent of frequency in the upper percentage of percolation samples, Cloisite30B renders solid-like behavior by retarding confined chains and tethered the relaxation of segments [20, 23].

The rheological percolation threshold occurs at 0.20% wt for MWCNTs, which can be attributed to the high ability of MWCNTs to interact with hard segment and strong confinement for chain mobility and high affinity nanoparticles to each other [24].

Figure 3 shows the comparison storage modulus (G') versus concentration, and it shows that MWCNTs exert a better influence on increasing modulus at very low concentrations, which can be attributed to excellent interaction with the hard segment and its high aspect ratio in contrast with Cloisite30B.

Effect of Nanoparticles on DSC Peaks

Figure 4 shows DSC thermogram for the neat TPU and the nanocomposites.

In the literature, three peaks were observed in the DSC thermogram of TPU. The first peak attributed to local restructuring of hard segment and the second peak is for the association and mixing of hard and soft segments, and the third peak occurs due to the melting of the nano- or microdomain of the hard segment in this TPU [11–13, 21, 25].

These peaks in DSC would change with the situation: For example, if annealing time increased, letting the hard segment to assemble together makes a hard domain, and the second peak to decrease and adding to the third peak [1, 20, 24].

There were three endothermic peaks in neat TPU. Similar results were reported for TPU by other literature, same as Koberstein and Russell [11].

In this work, in the presence of low Cloisite30B, no change was observed in three peaks. This is because nanoparticles have an affinity with soft segments, and second because the noncrystalline section has no change, but in the high presence of Cloisite30B, some nanoparticles attain the hard segment and act as a nucleating agent, creating a situation for the hard segment in noncrystalline section to move in the crystalline section and form a hard domain. In a low presence of Cloisite30B, it has no effect on phase separation and may even increases the intermixing between hard and soft segments. But in the high presence, it shows a nucleating effect.

As mentioned earlier, and surveyed in this work, the presence of MWCNTs or the low presence of MWCNTs has a strong affinity with the hard segment and causes the second peak to sharply decrease and adds to the third peak, helping the hard segment to move to the crystalline section and form a hard domain aggregation.

Dynamic Mechanical Analysis (DMA)

DMA is one of the best methods for studying the glass transition in polymers.

TPU the same as the other block copolymer has two distinct sections (hard and soft segments). For this reason, each section has a special glass transition.

Velankar and Cooper found that the glass transition for TPUs is around 50 to 130°C for the hard segment and -10 to -50°C for the soft segment. The glass transition temperature of the hard segment in neat TPU is around 110°C and the glass transition temperature for the soft segment is around -25°C.

Nanoparticles can cause confinement for TPU chains by interacting with soft segments, which are the main source of damping in the TPU. Hence, for nanocomposites increasing nanoparticle content, it leads to a decrease in $\tan(\delta)$ or the ability of the polymer chain to damp.

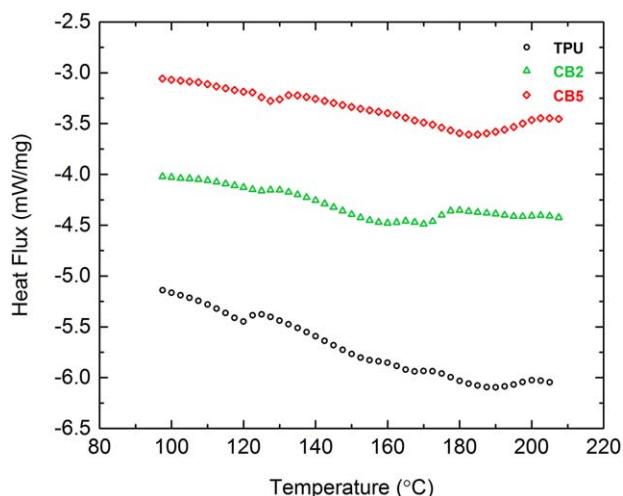


FIG. 4. Nonisothermal DSC thermograms for neat TPU and nanocomposite Cloisite30B samples obtained by heating ramp of 10°C/min. [Color figure can be viewed at wileyonlinelibrary.com]

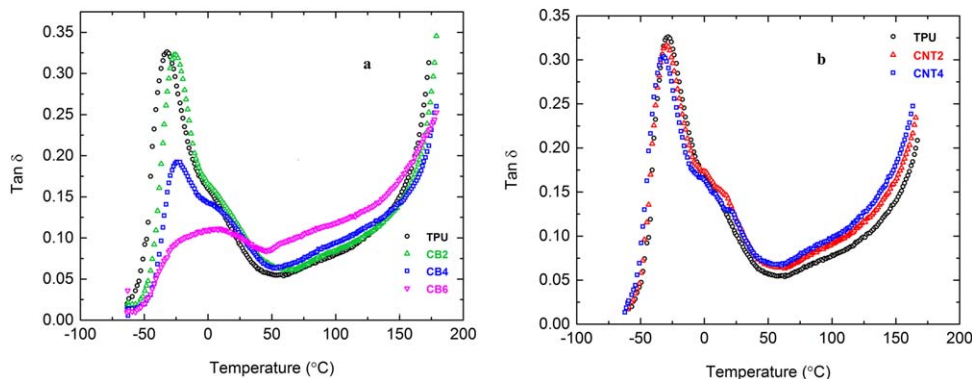


FIG. 5. Temperature dependence of the dynamic viscoelasticity $\tan(\delta)$: (a) TPU/Closite30B, (b) TPU/MWCNT. [Color figure can be viewed at wileyonlinelibrary.com]

Also, the peak of $\tan(\delta)$ displays the glass transition of the soft segment in neat TPU and nanocomposite samples [7, 20].

From the result shown in Fig. 5a and b, one can easily recognize that the decrease in the area of $\tan(\delta)$ of TPU is by increasing the content of the loading of Closite30B and MWCNTs. The peak of the $\tan(\delta)$ in the presence of Closite30B clearly shifts to the right. Assume this phenomenon is caused by the interaction of the soft segments with Closite30B, but in high amounts of this nanoparticle, this shift is slighter. As observed in the DSC test, Closite30B can move toward the hard segment and bring out from inside of the mixing phase of the hard and soft segments. As is clear in Fig. 5b, the addition of MWCNTs causes the glass transition temperature of the soft segment to decrease because nanoparticles interact with the hard segment and act as a nucleating agent and bring out from the interdomain mixing. They let the soft segment have better freedom of movement.

From the DMA and DSC results, understood that in the TPU/MWCNTs nanocomposites, the affinity between the MWCNTs and the hard segments is better, compared with the soft segments. The existence of the MWCNTs can act as a nucleating agent for hard domain aggregation.

TPU/Closite30B nanocomposite systems have a greater thermodynamic affinity between the Closite30B and the soft segments: Closite30B approximately does not affect the nucleation process at a high percentage.

Agreement Between RMS and DSC at Phase Separation Temperature

Finding the phase separation temperature is one of the challenging subjects in literature. In the DSC cooling scan, the first peak (from the right side) reveals the nucleation temperature and the second peak shows the growth of hard domains. In order to find the wide range of temperature in DSC and not the obvious point of this method, we try and find another reliable method.

Mourier et al. proposed a temperature sweep experiment with different cooling rate scans.

For the sake of easier comparison, we choose the same cooling rate ($10^{\circ}\text{C}/\text{min}$) for both DSC and rheological measurements.

Any change in the storage modulus slope arises from the phase separation and when the storage modulus (G') crosses the loss modulus (G''), it means that a few phase separations occur [15, 16, 23].

This experiment gives us better insights about the factors that could affect the phase separation temperature.

In an exothermic thermogram, the DSC first peak collaborates with nucleating hard domains and the second peak is because of the growth of hard domains. On using nanoparticles, the nucleating process increases, and the associated temperature shifts to the higher temperature.

For the neat TPU, both DSC and rheology tests acclaim that phase separation is around 110°C . For TPU/MWCNTs nanocomposite samples, the crystallization temperature was around 140°C at a cooling rate of $10^{\circ}\text{C}/\text{min}$ in both experiments. The increment of the crystallization temperature is because of the nucleating effect of MWCNTs. On the other hand, for TPU/Closite30B nanocomposite samples, no variation in the crystallization temperature was observed. Figure 6a–c shows the crystallization temperature for neat TPU, Closite30B, and MWCNTs nanocomposites, respectively. In this work, we observed Closite30B has an interaction with a soft segment, and does not play as a nucleating agent at low concentrations, but in the high content of Closite30B, this nanoparticle attains hard segments. Thereafter, the DSC nucleation peak shifts to higher temperatures. The nucleation effect of MWCNTs can be attributed to the high affinity of these nanoparticle to hard segments, which cause a shift in the DSC nucleation peak, even at low content (see Fig. 7a and b).

Effect of Nanoparticles on Temperature Sweep Test

Some investigators have made attempts to determine order-disorder transition (ODT) temperature (T_{ODT}) in

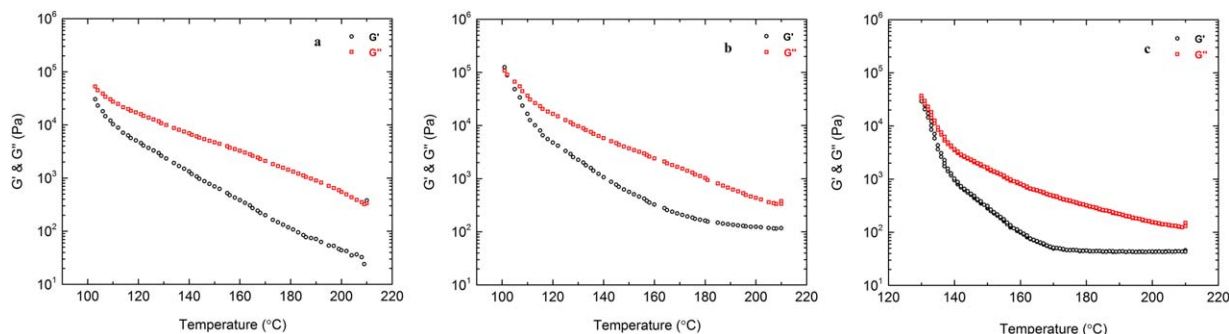


FIG. 6. Temperature sweep experiment on neat TPU (a), (b) CB2, (c) CNT2 at a constant cooling rate of 10°C/min. [Color figure can be viewed at wileyonlinelibrary.com]

TPUs using temperature sweep experiments. They used a rheological instrument for block copolymers, which proposed that the temperature at which G' begins to drop precipitously in temperature sweep experiment could be considered the T_{ODT} [11, 13, 14].

The first drop in G' versus temperature can be related to the destruction of the network that mainly resulted from the intersegmental mixing of noncrystalline hard microdomains with soft segments. The second transition where the G' and G'' cross each other is the temperature at which the three-dimensional network is completely destroyed and the crystalline microdomains are melted [26].

Hydrogen bonding takes place continuously in TPUs, making the phase boundary between hard and soft segments blurred, although the extent of hydrogen bonding becomes weaker with increasing temperatures [27].

The results of a similar experiment performed on neat TPU and nanocomposite samples with CB2 and CNT2 after being annealed at 160°C for 2 h, until the hard segment has opportunity to form a hard domain and a clear transition can be viewed, are shown in Fig. 8a and b.

For the neat TPU sample, two distinct drops were observed in the storage modulus, which can be related to the two mechanisms discussed above.

Between different samples, we selected CB2 and CNT2 samples that have fine phase separation, because in

high nanoparticle content, nanoparticle aggregation acts as a confinement for phase separation. In nanocomposite samples, we observed a smoothed drop in G' and G'' : We assume it is related to the ability of nanoparticles to interact with polymer chains. The high modulus nanoparticle prevents from dropping of modulus at high temperature.

Characterization of the Nucleating Ability Nanoparticle and Preshear

Most of the studies on flow-induced crystallization have been carried out on pure polymers. Though the combined effect of shear flow and nanoparticles on the crystallization of polymers has received considerable attention in recent years, the flow influence on the crystallization kinetics and changes in final morphology and properties. The flow effect in the presence of a nanoparticle nucleating agent decreased [10, 15, 16, 28].

However, it is difficult to accurately identify the synergistic effect of nanoparticle and preshear. Though some important aspects of flow-induced crystallization of particle-containing polymers have already been discerned, understanding and separating the two phenomena are still being debated.

Nanoparticle and shear flow effect on the phase separation TPU has been studied, but the co-existence of the

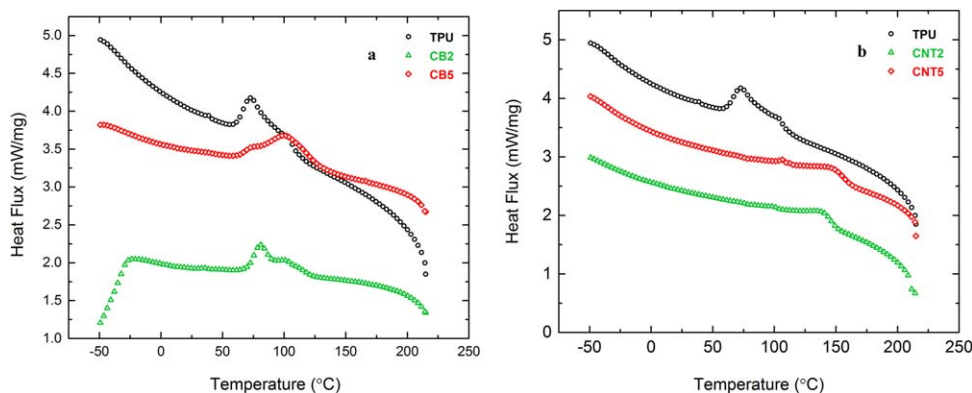


FIG. 7. DSC nonisothermal thermograms for (a) TPU/Closite30B, (b) TPU/MWCNT samples by cooling ramp of 10°C/min. [Color figure can be viewed at wileyonlinelibrary.com]

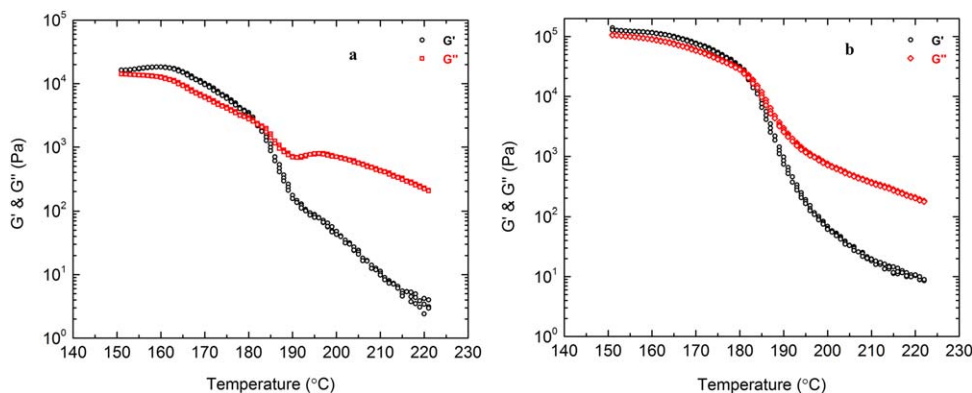


FIG. 8. Storage and loss modulus versus temperature for (a) neat TPU, (b) nanocomposite samples. [Color figure can be viewed at wileyonlinelibrary.com]

two factors has not been surveyed. In this study, we tried to separate the effects of these factors from each other. Toward this aim, while searching the literature, we found a formula for the different factor efficiencies which have an effect on the kinetics of phase separation.

In one of the articles, the nucleation efficiency calculated from DSC peak temperature result, $T_{c,NA}$, is the nucleation temperature in the presence of nanoparticles [8, 14, 19, 25].

The Lotz nucleating efficiency is defined by this formula:

$$NE = 100(\Delta T_{NA})/\Delta T = 100(T_{c,NA} - T_{c, \text{pure}})/(T_{c,nucMAX} - T_{c,pure}) \quad (1)$$

Also, ΔT is the difference between minimum and maximum nucleation temperatures of the neat polymer, and ΔT_{NA} is the difference between the minimum nucleation temperature of the neat polymer and the polymer with a certain amount of the particles in the DSC test.

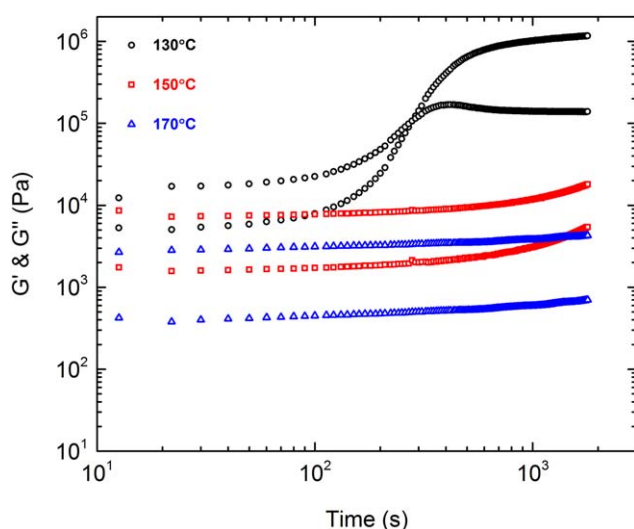


FIG. 9. Storage and loss modulus versus annealing time for neat TPU with different annealing temperatures. [Color figure can be viewed at wileyonlinelibrary.com]

As can be observed in Figs. 9 to 11 in the time sweep test, the effects of three factors—temperature, nanoparticle, and preshear were investigated.

In this study, we have used an isothermal time sweep test result to calculate the Lotz nucleating efficiency with this agreement that nucleation temperature ($T_{c,NA}$) is defined as the temperature at which crossover happens [storage modulus (G') crosses loss modulus (G''), and being the upper than it, in 2 h annealing time opportunity]. To ensure a good understanding of this issue, we ran a sweep experiment several times in order to quantify our result.

In neat polymer, minimally and maximally temperature found at 130°C, 170°C from time sweep test, which means in our annealing time, around 2 h shows that the storage modulus could cross the loss modulus. It is related to a three-dimensional network of hard domain form. In the presence of nanoparticles, this nucleation temperature shifted to upper temperatures for the nucleating effect of MWCNTs and Closite30B: the fastest kinetics of phase separation occur in CB2 and CNT2 samples

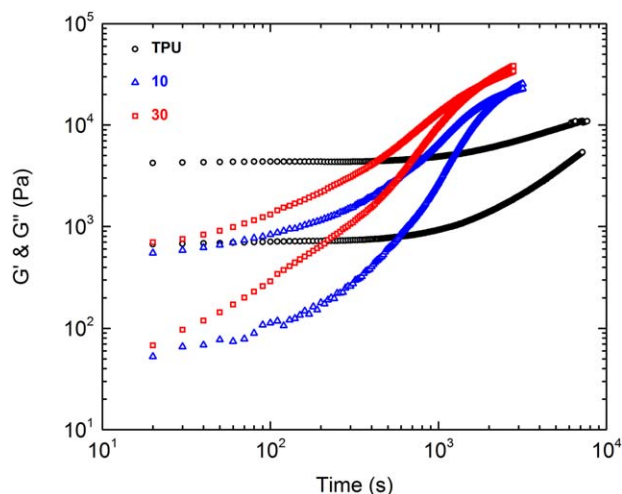


FIG. 10. Storage and loss modulus versus annealing time for neat TPU with different preshears. [Color figure can be viewed at wileyonlinelibrary.com]

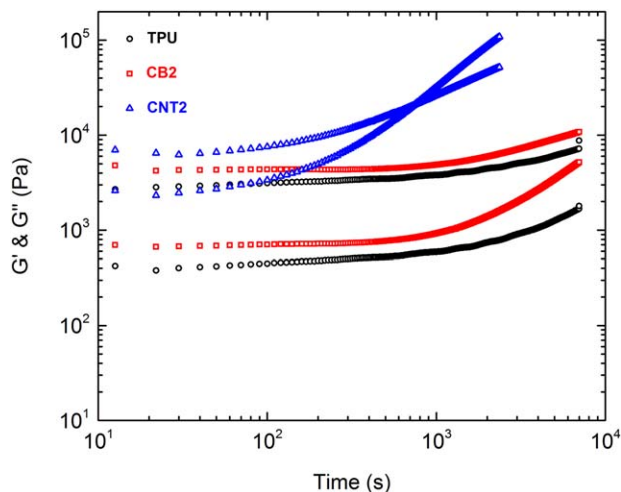


FIG. 11. Storage and loss modulus versus annealing time for neat TPU with different nanoparticles. [Color figure can be viewed at wileyonlinelibrary.com]

because the upper percolation threshold aggregation of nanoparticle decreases this kinetic.

In preshear samples, at the first drop, the storage modulus broke any structure in the polymer—the same hard microdomain structure and the nanoparticle structure and then promoted the kinetics of the phase separation with the orientation of the hard segment. In this work, we applied a preshear from a 5 to 30 s⁻¹ range and observed with increasing preshear, the kinetic phase separation increased.

In nanocomposite samples, MWCNTs nanoparticles exert a great effect on phase separation kinetics, but Closite30B does not have a tangible effect. When we applied a preshear, it has a great effect on Closite30B nanocomposite samples, because of the lower nucleating effect of this nanoparticle in comparison with MWCNTs. At around the percolation threshold, the formation of three networks of nanoparticle caused the increment in the storage modulus and brought a hindrance effect for hard segment aggregation. When applied, preshear ruins nanoparticle aggregation and induces the formation of hard segment microdomains.

Nanoparticles have a nucleating agent and preshear increases microphase separation kinetics with hard

TABLE 2. Effect of different factors on percentage of crystallization.

Sample	Driving force	Percentage of crystallization (%)
Low shear	$\Delta T = 5^\circ\text{C}$	16.6
High shear	$\Delta T = 15^\circ\text{C}$	50
Closite30B	$\Delta T = 5^\circ\text{C}$	16.6
MWCNTs	$\Delta T = 22.5^\circ\text{C}$	75
Low shear + Closite30B	$\Delta T = 10^\circ\text{C}$	33.3
High shear + Closite30B	$\Delta T = 15^\circ\text{C}$	50
Low shear + MWCNTs	$\Delta T = 22.5^\circ\text{C}$	75
High shear + MWCNTs	$\Delta T = 25^\circ\text{C}$	83.3

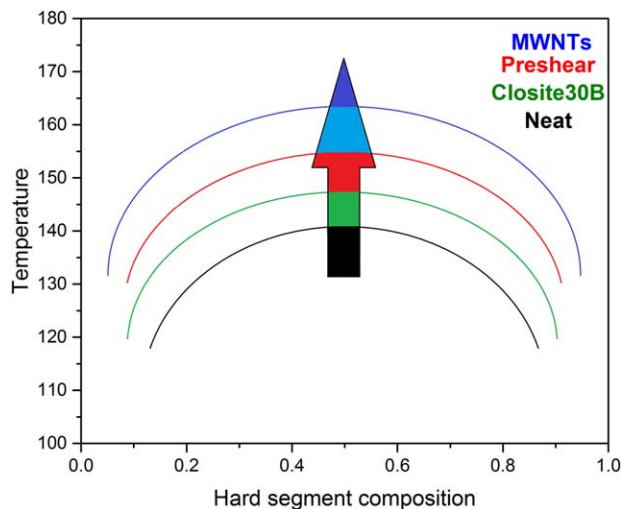


FIG. 12. Schematic phase diagram: nanoparticles and preshear effect on UCST phase diagram. [Color figure can be viewed at wileyonlinelibrary.com]

segment orientation. The calculated Lotz efficiency for Closite30B is 10%, for MWCNTs 80% and, for preshear, it is 40%. The table calculated the Lotz efficiency in different situations low and high percentages of nanoparticle with or without preshear. This is listed in Table 2.

With this formula and percentage of nucleating efficiency that could be considered, we can separate the effects of different factors on the kinetics of phase separation on TPUs.

In the survey in literature, it is understood that block copolymers, such as TPUs, have an upper critical solution temperature (UCST) contrary to other polymers. In this work, for better comprehension, we draw a UCST schematic phase diagram, temperature versus hard segment composition (HS).

As observed above, each factor has a special effect on phase separation kinetics. For this reason, we collected these different influences in Fig. 12. It is observed the MWCNTs, preshear, and Closite30B, respectively, cause shifting of the phase diagram to upper temperatures.

CONCLUSIONS

In this article, a systematic investigation of the combined effect of the presence of nanoparticle and preshear on the microphase separation or crystallization of TPUs nanocomposite has been surveyed.

The results showed that the kinetics of the phase separation of thermoplastic polyurethane have physical similarities with the kinetics of the crystallization process.

The kinetics of the phase separation at high preshear and lower percentage of nanoparticle increased, while it showed a decrease in higher compositions. The nucleation effect of nanoparticle and preshear with the orientation of hard segment increases the kinetics of phase separation of soft and hard segments.

The thermal analysis of DSC showed that multiple endothermic peaks of thermoplastic polyurethane were affected in the presence of nanoparticles.

DMA tests showed that Closite30B has an affinity with the soft segment and MWCNTs with the hard segment, which is in agreement with DSC and rheological experiments. Finally, it has been shown that at low values of the preshear, nucleation by the nanoparticle accelerates the crystallization kinetics. However, at sufficiently large values of the preshear, flow will dominate the nucleation. Hence, the kinetics was found to be independent of nanoparticles and concentration.

Preshear and nanoparticles can accelerate phase separation kinetics, but the effect of preshear on the kinetics of phase separation was reduced in the presence of MWCNTs. At around the percolation threshold, hard domain formation and nanoparticle network assembly together faced a challenge, but preshear gave more time to the hard domain assemblies with the dispersion of nanoparticles. A generic framework based on the additivity of the presence of nanoparticles and flow is presented to explain how both effects contribute to the crystallization process. However, the additive rule of flow and the presence of particles are not a general feature.

REFERENCES

1. C.D. Han, *Rheology and Processing of Polymeric Materials: Polymer Rheology*. Oxford University Press, UK (2007).
2. P.J. Stenhouse, S.W. Kantor, and W.J. MacKnight, *Macromolecules*, **22**, 1467 (1989).
3. M. Shahrousvand, G. Mir Mohammad Sadeghi, and A. Salimi, *J. Biomater. Sci. Polym. Ed.* **27**, 1 (2016).
4. M. Shahrousvand, G. Mir Mohammad Sadeghi, E. Shahrousvand, M. Ghollasi, and A. Salimi, *Colloids Surf. B*, **156**, 292 (2017).
5. S. Velankar and S.L. Cooper, *Macromolecules*, **31**, 9181 (1998).
6. S. Velankar and S.L. Cooper, *Macromolecules*, **15**, 71 (1982).
7. P. Pokharel, *Chem. Eng. J.*, **253**, 356 (2014).
8. B. Xu, W.M. Huang, Y.T. Pei, Z.G. Chen, A. Kraft, R. Reuben, J.Th.M. De Hosson, and Y.Q. Fu, *Eur. Polym. J.*, **45**, 1904 (2009).
9. M. Song, H.S. Xia, K.J. Yao, and D.J. Hourston, *Eur. Polym. J.*, **41**, 259 (2005).
10. M. D'Haese, P. Van Puyvelde, and F. Langouche, *Macromolecules*, **43**, 2933 (2010).
11. J.T. Koberstein and T.P. Russell, *Macromolecules*, **19**, 714 (1986).
12. L.M. Leung and J.T. Koberstein, *Macromolecules*, **19**, 706 (1986).
13. A.J. Ryan, C.W. Macosko, and W. Bras, *Macromolecules*, **25**, 6277 (1992).
14. A. Saiani, C. Rochas, G. Eeckhaut, W. Daunch, J.W. Leenslag, and J. Higgins, *Macromolecules*, **37**, 1411 (2004).
15. E. Mourier, L. David, P. Alcouffe, C. Rochas, F. Méchin, and R. Fulchiron, *J. Polym. Sci. Part B: Polym. Phys.*, **49**, 801 (2011).
16. E. Mourier, R. Fulchiron, and F. Méchin, *J. Polym. Sci. Part B: Polym. Phys.*, **48**, 190 (2010).
17. D. Wu, L. Wu, L. Wu, and M. Zhang, *Polym. Degrad. Stab.*, **91**, 3149 (2006).
18. A. Barick and D. Tripathy, *J. Appl. Polym. Sci.*, **117**, 639 (2010).
19. Y. Tien and K. Wei, *Polymer*, **42**, 3213 (2001).
20. T. Hosseini-Sianaki, H. Nazockdast, B. Salehnia, and E. Nazockdast, *Polym. Eng. Sci.*, **55**, 2163 (2015).
21. H. Koerner, J.J. Kelley, and R.A. Vaia, *Macromolecules*, **41**, 4709 (2008).
22. S. Velankar and S.L. Cooper, *Macromolecules*, **33**, 395 (2000).
23. B. Ranjbar and H. Nazockdast, *J. Appl. Polym. Sci.*, **132**, (2015).
24. B. Finnigan, D. Martin, P. Halley, R. Truss, and K. Campbell, *J. Appl. Polym. Sci.*, **97**, 300 (2005).
25. J.-B. Zeng, F. Wu, C.L. Huang, Y.S. He, and Y.Z. Wang, *ACS Macro Lett.*, **1**, 965 (2012).
26. J.G. Kennemur, M.A. Hillmyer, and F.S. Bates, *ACS Macro Lett.*, **2**, 496 (2013).
27. S. Awad, H. Chen, G. Chen, X. Gu, J.L. Lee, E. Abdel-Hady, and Y.C. Jean, *Macromolecules*, **44**, 29 (2010).
28. M. D'Haese, F. Langouche, and P. Van Puyvelde, *Macromolecules*, **46**, 3425 (2013).